0026-895X/90/060805-11$03.00/0

MOLECULAR PHARMACOLOGY, 38:805-815

Characterization of Muscarinic M_4 Binding Sites in Rabbit Lung, Chicken Heart, and NG108-15 Cells

SEBASTIAN LAZARENO,[1] NOEL J. BUCKLEY, and FIONA F. ROBERTS[2]

Department of Neuropharmacology, Glaxo Group Research Ltd., Ware, Hertfordshire SG12 0DJ, United Kingdom (S.L., F.F.R.), and National Institute for Medical Research, Mill Hill, London NW7 1AA, United Kingdom (N.J.B.)

Received July 3, 1990; Accepted September 11, 1990

SUMMARY

We have carried out an extensive pharmacological characterization of muscarinic binding sites in rabbit lung and chicken heart in parallel with M_1, M_2, and M_3 sites. [^{3}H]Pirenzepine, a selective antagonist at M_1 receptors, bound saturably and reversibly to membranes from chicken heart and rabbit lung. These binding sites were not M_1 receptors, however, because the cardioselective antagonist himbacine had 10-fold higher affinity at these sites than at [^{3}H]pirenzepine sites in rat and rabbit cortex (true M_1 sites). We measured the inhibitory potency of 28 antagonists at [^{3}H]*N*-methylscopolamine-labeled sites in chicken heart, rabbit lung, rat heart (M_2 sites), and rat submandibular gland (M_3 sites) and at M_1 sites in rat cortex. The sites in rabbit lung were different from M_1, M_2, and M_3 sites, because they had moderate to high affinity for M_1-selective compounds (pirenzepine and telenzepine), M_2-selective compounds (himbacine and methoctramine), and M_3-selective compounds (hexahydrosiladifenidol and 4-diphenylacetoxy-*N*-methylpiperidine methiodide). The sites in chicken heart resembled most those in rabbit lung, with similar high affinity for secoverine, but they were not the same because tropicamide, diphenylacetoxybutynyl dimethylamine, and [^{3}H]-*N*-methylscopolamine were more potent in rabbit lung. In a further series of experiments, we compared the affinity of six of the most discriminating antagonists in membranes from rabbit lung and NG108-15 cells, a neuroblastoma-glioma cell line reported to express the muscarinic m4 receptor gene. The antagonists had very similar affinities in the two tissues, the largest discrepancy being that pirenzepine was twice as potent in rabbit lung as in NG108-15 cells. Northern blots using probes designed to discriminate between five species of muscarinic receptor RNA detected only m4 mRNA in rabbit lung. We conclude that rabbit lung contains a muscarinic M_4 binding site with a quite distinctive pharmacology and that chicken heart contains a receptor with similarities to the M_4 sites. This is the first report to characterize native M_4 binding sites in a nonneuronal mammalian tissue.

At least five structurally distinct subtypes of muscarinic receptor are expressed in mammalian tissue (1–4). The m1, m2, and m3 genes probably encode the pharmacologically defined M_1, M_2, and M_3 receptors (2, 5–8). The receptor encoded by the m4 gene may have pharmacological similarities to both M_1 and M_2 receptors; muscarinic binding sites in oocytes or Chinese hamster ovary cells transfected with the m4 gene have a relatively high affinity for PRZ, the antagonist that pharmacologically defines M_1 receptors (9, 10), and the m4 receptor has greatest homology with the m2 receptor found in mammalian heart (1, 2). Like the m2 receptor, and unlike the m1 and m3 receptors, the m4 receptor mediates an inhibition of adenylyl cyclase when expressed in transformed fibroblasts (11). We wondered whether some of the 'atypical' M_1 receptors already described in the literature might be M_4 receptors. Chick heart contains receptors with relatively high affinity for PRZ but that mediate inhibition of adenylyl cyclase (12), and rabbit peripheral lung contains 'M_1' binding sites with a somewhat higher affinity for the cardioselective antagonist AF-DX116 than that of M_1 sites in cortex (13). The available pharmacological data concerning the m4 receptor (10) do not provide any firm criteria for testing the hypothesis that one or both of these atypical sites are M_4 sites. We have, therefore, characterized the muscarinic binding sites in chicken heart and rabbit peripheral lung, together with M_1, M_2, and M_3 sites, using a wide range of antagonists. We identified six compounds that clearly distinguish between rabbit lung and the other tissues, and we used these compounds to compare the sites in rabbit lung with those in NG108-15 cells, a mouse-rat neuroblastoma-glioma cell line (14) reported to express only the m4 receptor (2). In addition, we have used Northern blot analysis to detect the muscarinic receptor transcripts expressed in rabbit lung. We

[1] Present address: MRC Collaborative Centre, 1–3 Burtonhole Lane, Mill Hill, London, NW7 1AD, UK.
[2] Present address: Department of External Scientific Affairs, Glaxo Group Research Ltd., Greenford, London, UK.

ABBREVIATIONS: PRZ, pirenzepine; NMS, *N*-methylscopolamine; HSD, hexahydrosiladifenidol; 4-DAMP, 4-diphenylacetoxy-*N*-methylpiperidine methiodide; DABDMA, diphenylacetoxybutynyl dimethylamine HBr; PrBCh, propyl benzilyl choline; HEPES, 4-(2-hydroxyethyl)-1-piperazineethanesulfonic acid; Gpp(NH)p, guanyl-5′-yl imidodiphosphate; m1–m5, structurally defined muscarinic receptors; M_1–M_4, pharmacologically defined muscarinic receptors; SDS, sodium dodecyl sulfate; kb, kilobases.

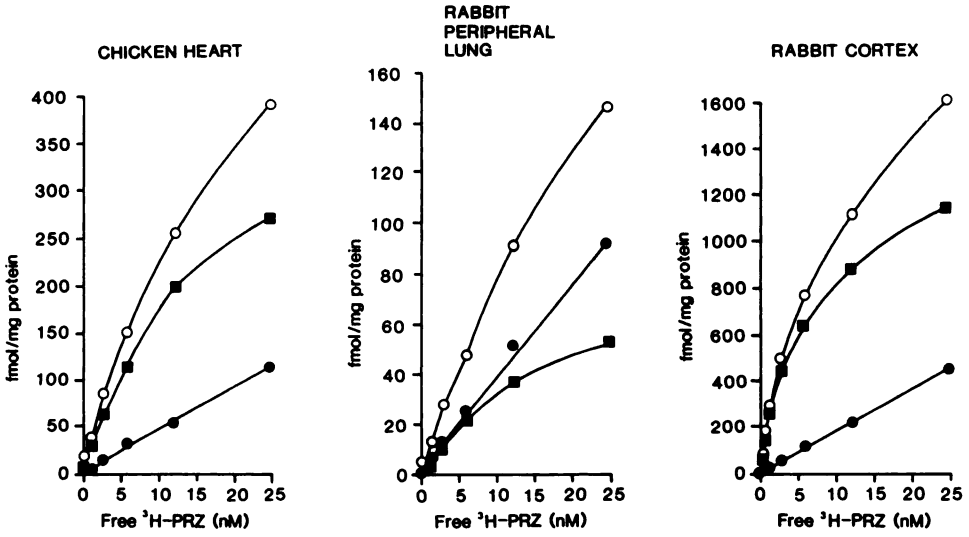

Fig. 1. [³H]PRZ saturation curves in chicken heart, rabbit peripheral lung, and rabbit cortex membranes. Membranes were incubated with [³H]PRZ for 2 hr and collected by filtration. Specific binding (■) is the difference between binding obtained in the absence (○) and presence (●) of 1 μM atropine. The data are from a single experiment conducted in triplicate.

TABLE 1

[³H]NMS saturation data

Membranes were incubated with [³H]NMS for 2 hr. Nonspecific binding was measured in the presence of 1 μM atropine. The specific binding was analyzed by the program LIGAND according to a one-site model.

	Rat heart (M_2)	Rat gland (M_3)	Chicken heart	Rabbit lung
n	5	5	16	22
K_d (pM)	206 ± 19	67 ± 2	198 ± 12	62 ± 5
B_{max} (pmol/g of weight)	7.8 ± 0.4	7.4 ± 0.6	35 ± 2	4.7 ± 0.4

conclude that rabbit lung contains M_4 sites with a distinctive pharmacology that is similar, but not identical, to that of chicken heart sites.

Materials and Methods

Cell culture. NG108-15 cells were obtained from Prof. D. Brown, University College (London). They were grown at 37.5° in T175 Nuclon tissue culture flasks as a monolayer, under an atmosphere of humidified 5% CO_2 in air. The growth medium was Dulbecco's modified Eagle's medium containing 10% fetal calf serum, 100 μM hypoxanthine, 1 μM aminopterin, and 16 μM thymidine. The cells were seeded at a density of 10^6 cells/175 cm^2, grown until 60–90% confluent (usually 3–4 days), and reseeded at the same density. They were harvested by replacement of the medium with phosphate-buffered saline, followed 15 min later by centrifugation at 1000 × *g* for 5 min.

Membrane preparation. Cerebral cortex, heart (mainly ventricles), and submandibular gland were obtained from male Lister Hooded rats. Heart ventricles were obtained from 6–12-week-old White Leghorn/Rhode Island Red chickens. Lungs and cerebral cortex were removed from New Zealand White rabbits. The edges of the lungs were cut to a depth of 1–2 cm and the parenchyma from the surface of the remainder of the lungs was trimmed to a depth of about 3 mm, the remaining lung tissue containing large airways was discarded. The tissues were dissected on ice and cut into small pieces. All the tissues were homogenized in 10–20 volumes of iced homogenizing buffer (20 mM Na·HEPES, 10 mM Na_2EDTA, pH 7.2), using three to five 5-sec bursts with an UltraTurrax homogenizer. The peripheral tissues were filtered through a course nylon mesh and all the homogenates were centrifuged at 40,000 × *g* for 12 min, resuspended in assay buffer (20 mM Na·HEPES, 100 mM NaCl, 0.5 mM Na_2EDTA, pH 7.4) at a concentration of 200 mg of wet weight/ml, and frozen in 1-ml aliquots at −70°.

Binding assays. Frozen membranes were resuspended in assay buffer with the following tissue concentrations (mg of wet weight/ml): cortex, 1.6; rat heart, 2; rat gland, 1.2; chicken heart, 1; and rabbit lung, 2.3. Three milliliters of membranes were incubated with antagonists and radioligand at 22° for 2 hr or as stated. The membranes were

TABLE 2

Kinetic parameters of [³H]PRZ and [³H]NMS

Association and dissociation experiments were conducted as described in Materials and Methods and were analyzed using the method of Bennett (57). K_{-1} (the dissociation rate constant) is the slope of the regression line of the plot in (B_t/B_0), where B_0 is specific binding before addition of excess atropine and B_t is the specific binding *t* min after atropine addition. $t_{½}$ is the time for 50% association or dissociation, derived from $t_{½} = \ln(2)/K$. K_{+1} (the association rate constant) was derived from the equation $K_{+1} = (K_{obs} - K_{-1})/[L]$, where $[L]$ is the radioligand concentration and K_{obs} is the slope of the regression line of $\ln(B_{eq}/(B_{eq} - B_t))$, where B_{eq} is specific binding at equilibrium and B_t is specific binding *t* min after the addition of membranes to radioligand. K_d (the dissociation constant) = $K_{-1}/K_{+1} \times 1000$.

Ligand/tissue	Dissociation			Association			
	n	K_{-1}	$t_{½}$	*n*	$t_{½}$	K_{+1}	K_d
		$min^{-1} \times 10^{-3}$	*min*		*min*	$min^{-1} \times nM^{-1} \times 10^{-2}$	pM
[³H]PRZ							
Rat cortex	3	43 ± 1	16.2 ± 0.2				
Rabbit cortex	2	27 ± 3	25.8 ± 2.8				
Rabbit lung	3	59 ± 3	11.8 ± 0.4				
Chicken heart	2	96 ± 20	7.5 ± 1.5				
[³H]NMS							
Rat heart	7	272 ± 20	2.7 ± 0.2	1	1.6	25	1270
Rat gland	3	16 ± 1	43 ± 2	2	12 ± 4	12 ± 5	175 ± 76
Chicken heart	4	135 ± 10	5.2 ± 0.4	3	3.4 ± 0.5	29 ± 7	542 ± 110
Rabbit lung	6	40 ± 2	18 ± 1	3	5.9 ± 0.7	37 ± 1	108 ± 5
NG108-15	3	22 ± 2	32 ± 3	3	4.6 ± 0.8	62 ± 4	35 ± 3

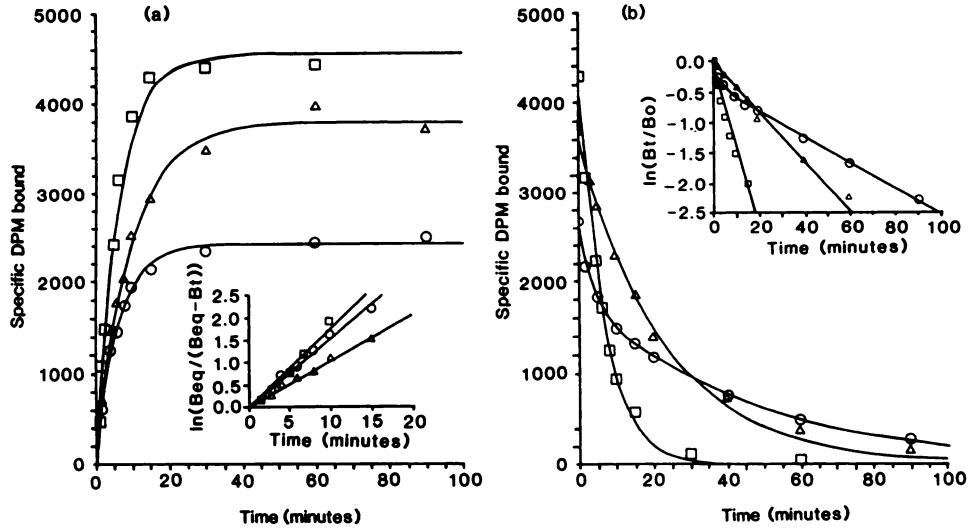

Fig. 2. Association (a) and dissociation (b) of [^{3}H]NMS (0.2 nM) in membranes from chicken heart (□), rabbit lung (△), and NG108-15 cells (○). For association curves, the membranes were incubated with [^{3}H]NMS for the indicated times before filtration. For dissociation curves, the membranes were incubated with [^{3}H]NMS for 60 min (chicken heart) or 90 min and filtered at the indicated times after addition of 1 μM atropine. In all cases, some tubes contained 1 μM atropine from the outset, and this nonspecific binding (about 100 dpm) has been subtracted from the rest of the data to yield specific binding. The *lines* for the association data and for the dissociation data from chicken heart and rabbit lung show the fit to a single exponential function. The dissociation data from NG108-15 membranes have been fitted to a two-component exponential function. *Insets*, linearizing transformation of the data, using $\ln(B_{eq}/(B_{eq}-B_t))$ for association curves and $\ln(B_t/B_0)$ for dissociation curves, where B_t is the binding at time t, B_{eq} is the binding at equilibrium, and B_0 is the binding at the start of the dissociation; B_{eq} and B_0 were derived from the curve-fitting procedure. The data were obtained in a single experiment conducted in triplicate.

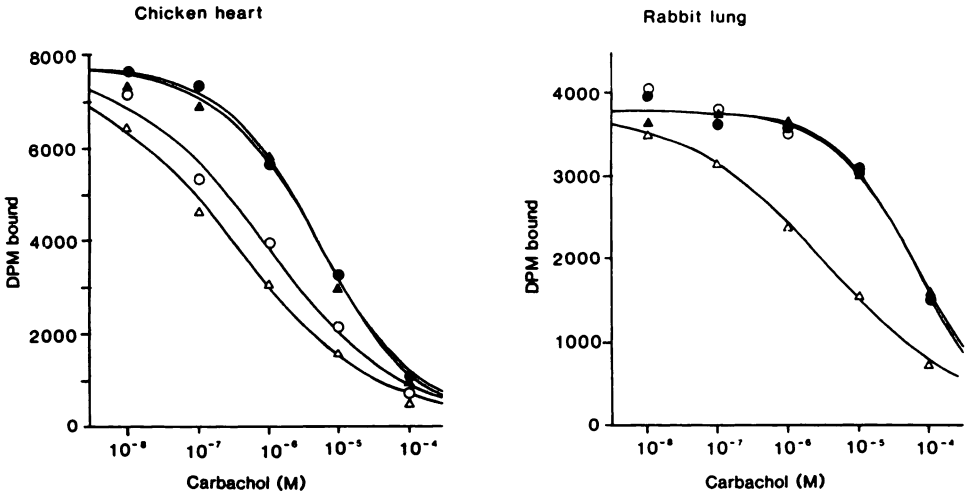

Fig. 3. Inhibition by carbachol of total [^{3}H]NMS (0.2 nM) binding to chicken heart and rabbit lung membranes in the presence of no additions (○), 0.1 mM Gpp(NH)p (●), 10 mM $MgCl_2$ (△), or Gpp(NH)p and $MgCl_2$ (▲). The data are from a single experiment conducted in duplicate, which was repeated with almost identical results.

collected by filtration and washed with 2 × 3 ml of 0.9% iced saline, using a Brandel cell harvester and Whatman GF/B glass fiber filter strips previously soaked in 0.1% polyethylenimine and dried before use, and were counted for radioactivity at an efficiency of about 40%. Nonspecific binding was measured in the presence of 1 μM atropine.

In competition studies, fixed concentrations of 0.1–0.2 nM [^{3}H]NMS or 0.5–1 nM [^{3}H]PRZ were used, except in experiments involving [^{3}H]PRZ and rabbit lung or chicken heart, in which case fixed [^{3}H]PRZ concentrations of 1.3 or 5 nM were used. Saturation studies usually contained nine radioligand concentrations spanning a 200-fold concentration range. Association experiments with [^{3}H]NMS were conducted by incubating membranes with 0.2–0.4 nM radioligand for various times before filtration. Dissociation experiments were conducted by incubating membranes with radioligand for 60–90 min. At that time, 10–30 μl of atropine were added to each tube to give a final atropine concentration of 1 μM, and the incubation mixture was filtered at various times thereafter. A 1-ml incubation volume was used in dissociation experiments with [^{3}H]PRZ. Experiments with [^{3}H]NMS were conducted in duplicate and those with [^{3}H]PRZ were conducted in duplicate or triplicate.

At one stage in the experiments, the K_d of [^{3}H]NMS in rabbit lung decreased to about 60% of its previous value when a new batch of [^{3}H]NMS was used. This may be related to the racemization reported to occur with [^{3}H]NMS (15). This change should not affect pK_i values, because IC_{50} values were usually transformed using the K_d value obtained in the same experiment. Most K_d estimates with chicken heart and rabbit lung used the first batch of [^{3}H]NMS; the second batch was used for M_2, M_3, and NG108-15 and paired rabbit lung K_d estimates. Some inhibition assays in rat heart contained 3 mM $MgCl_2$ and 0.1 mM guanosine triphosphate; the inclusion of these agents had no effect on the affinity of the antagonists.

Northern blot analysis. Samples of rabbit lung were rapidly dissected, frozen in liquid nitrogen, and stored at −70° for up to 2 months before RNA extraction. Frozen tissue was powdered in a slurry of liquid N_2 and total cellular RNA was extracted (16). Purity was assessed by A_{260}/A_{280} measurements and 15-μg samples were applied to 1% denaturing agarose gels (containing 2% formalin), electrophoresed, and electroblotted onto Genescreen (NEN). Blots were prehybridized overnight at 37° in buffer containing 4× standard saline-phosphate-EDTA

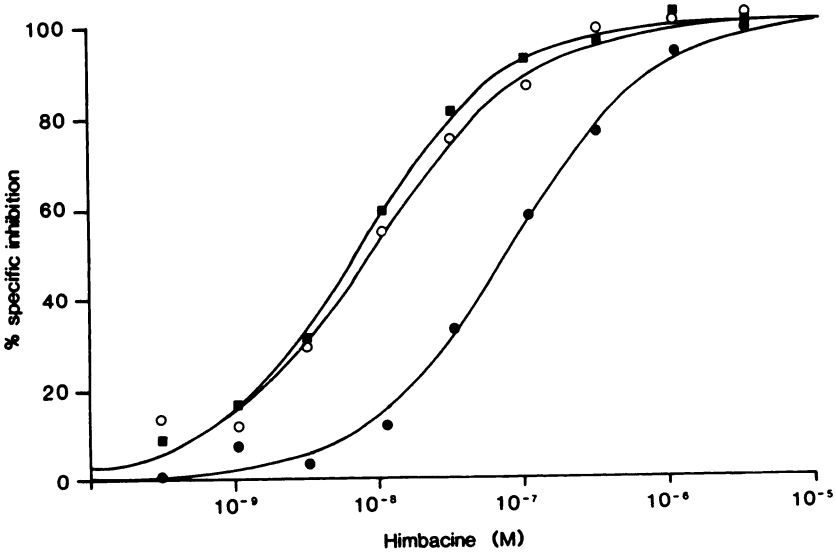

Fig. 4. Inhibition by himbacine of [^{3}H]PRZ binding to membranes from chicken heart (■), rabbit lung (○), and rat cortex (●). Membranes were incubated for 2 hr with 1.3 nM [^{3}H]PRZ and various concentrations of himbacine. Nonspecific binding was measured in the presence of 1 μM atropine. The data were obtained in a single experiment conducted in triplicate.

(150 mM NaCl, 10 mM NaH_2PO_4, 1 mM EDTA), 5× Denhardt's, 250 μg/ml yeast tRNA, 500 μg/ml denatured salmon sperm DNA, and 0.1% SDS). ^{32}P-tailed oligonucleotide probes were then added (2×10^6 dpm/ml) and hybridization was carried out at 37° overnight. Blots were washed (4 × 15 min) in 1× standard saline-phosphate-EDTA containing 0.1% SDS, at 55°, before apposition to Kodak XAR-5 film for 10 days. After exposure, blots were stripped in boiling 1% SDS before subsequent rehybridizations.

Oligonucleotide probe labeling. Probes consisted of an equimolar mixture of three antisense oligonucleotides (45- or 48-mers) corresponding to N-terminal, i3 cytoplasmic loop, and C-terminal domains of the rat m1—m5 muscarinic receptors. Probes were designed that shared minimum sequence identity among different receptor subtypes but that shared maximum homology with human cognate sequences. Sequences are taken from (Refs. 1, 3, and 17) and correspond to bases 31–79, 1056–1104, and 1299–1347 (m1); 49–97, 886–934, and 1076–1124 (m2); 1–48, 968–1016, and 1696–1744 (m3); 10–58, 866–914, and 1139–1187 (m4); and 641–689, 1164–1212, and 1265–1313 (m5). The degree of mismatch with human sequences varied between 0 and 4 bases. This design rationale was aimed at optimizing recognition of interspecies cognate sequences.

Probes were 3′-tailed with [^{32}P]dATP (111 TBq/mmol; NEN) using terminal deoxynucleotidyl transferase (BRL). A molar ratio of 1:10 oligonucleotides/[^{32}P]dATP was used to generate probes with a specific activity of approximately 4×10^9 dpm/μg of DNA, corresponding to a mean tail length of about 10 bases.

Data analysis. Kinetic experiments were analyzed as described in the legend to Table 2 and with a nonlinear fitting procedure in the RS1 package (BBN Software Products Corp.). Saturation curves were analyzed with the program LIGAND (18). In some saturation experiments with [^{3}H]NMS, nonspecific binding was estimated by the program. Saturation data were always best fitted by a one-site model. Inhibition curves were analyzed by the logistic curve-fitting program ALLFIT (19), to yield IC_{50} and slope values. K_i (M) values obtained from IC_{50} values (20)are the best estimates of the concentration of antagonist that would have occupied 50% of the sites had the radioligand not been present. They can only be considered as affinity estimates when the slopes of the inhibition curves are unity. The values are expressed as pK_i ($-\log K_i$).

Statistics. Models in the curve-fitting procedures were compared with the 'extra sum of squares' F test (18). Parameters are reported as arithmetic means and standard errors. When the number of observations (n) = 2, the standard error is equal to the range/2. Due to the large number of possible comparisons in this study, we have only performed statistical tests for particular comparisons of interest. The significant differences we report were derived from t tests, paired or unpaired (assuming equal variances) as appropriate, and taking $p < 0.05$ as the criterion for statistical significance.

Materials. The following compounds were purchased: [^{3}H]NMS (72–85 Ci/mmol) from Amersham; [^{3}H]PRZ (85–87 Ci/mmol) from New England Nuclear; carbachol, guanosine triphosphate, Gpp(NH)p, atropine, eucatropine, homatropine, orphenadrine, piperidolate, PRZ, and scopolamine from Sigma; and methoctramine from Semat. We are grateful for the following gifts: 4-DAMP and DABDMA (Dr. R. Barlow, University of Bristol); himbacine (Prof. W. Taylor, University of New South Wales); HSD (Prof. R. Tacke, University of Karlsruhe); PrBCh (Dr. N. Birdsall, NIMR, London); aprophen (Dr. P. Chiang, Walter Reed); secoverine (Duphar); benzhexol (Lederle); benztropine (MSD); biperiden (Knoll); botiacrine (Siegfried); BTM1086 (Maruko); cyclopentolate (Smith & Nephew); dicyclomine (Merrel Dow); oxybutinin (Marion Laboratories); procyclidine (Wellcome); telenzepine (Byk Gulden); and tropicamide (Smith & Nephew). CCI19234 (5-[(4-methyl-1-piperazinyl)acetyl]-5,10-dihydro-11*H*-dibenzo[b,e][1,4]diazepin-11-one), a pirenzepine analogue (21), and ipratropium were synthesized in our laboratories.

Results

Saturation studies. [^{3}H]PRZ bound to membranes from rabbit cortex, rabbit lung, and chicken heart. Within the concentration range used of 0.2–25 nM, the atropine-specific component of [^{3}H]PRZ binding was apparently saturable (Fig. 1) [^{3}H]PRZ had similar pK_d values in chicken heart (7.4 ± 0.3, n = 2) and rabbit lung (7.4 ± 0.2, n = 2) and was about 3-fold more potent in rabbit cortex (pK_d = 8.1, n = 1). The apparent density of [^{3}H]PRZ sites in rabbit lung (4 ± 1 pmol/g of weight) was less than one tenth the density in chicken heart (52 ± 13 pmol/g of weight) or rabbit cortex (79 pmol/g of weight). A very small amount of atropine-displaceable [^{3}H]PRZ binding was found in NG108-15 cell membranes (20% of total binding at 20 nM; none at concentrations of <17 nM), which was not characterized further.

[^{3}H]NMS bound specifically and saturably to an apparently homogeneous population of sites in all the tissues studied. Nonspecific binding was 10% or less of total binding. The K_d of [^{3}H]NMS was similar in rat and chicken heart and 3- to 10-fold less in rat gland, rabbit lung, and NG108-15 membranes (Table 1; see also Table 5). The density of [^{3}H]NMS sites in rabbit lung and chicken heart was similar to the values found with [^{3}H]PRZ, described above.

TABLE 3

Mean pK_i ± standard error and slope ± standard error values at five muscarinic binding sites

M_1 sites were labeled in rat cortex with [^{3}H]PRZ; [^{3}H]NMS labeled the other sites (M_2 sites in rat heart, M_3 sites in rat submandibular gland). Inhibition curves obtained in the presence of 0.5 nM [^{3}H]PRZ or 0.1–0.2 nM [^{3}H]NMS were analyzed by the program ALLFIT. IC_{50} values at M_1 sites are assumed to be K_i values. IC_{50} values at [^{3}H]NMS-labeled sites were converted to K_i values using the equation of Cheng and Prusoff (20).

Drug	pK_i/slope values				
	M_1	M_2	M_3	Chicken heart	Rabbit lung
PRZ	8.02 ± 0.08	6.48 ± 0.01	7.09 ± 0.05	7.60 ± 0.03	7.47 ± 0.04
	0.96 ± 0.02	0.91 ± 0.03	0.89 ± 0.01	0.89 ± 0.06	0.91 ± 0.04
Himbacine	7.16 ± 0.04	8.34 ± 0.02	7.09 ± 0.02	8.20 ± 0.07	8.21 ± 0.05
	0.84 ± 0.03	1.00 ± 0.03	0.96 ± 0.02	1.05 ± 0.04	0.85 ± 0.02
Methoctramine	7.60 ± 0.14	8.34 ± 0.09	6.88 ± 0.06	7.86 ± 0.05	7.81 ± 0.01
	0.79 ± 0.03	0.99 ± 0.04	0.96 ± 0.05	0.99 ± 0.04	0.84 ± 0.03
DABDMA	7.87 ± 0.02	6.65 ± 0.01	8.00 ± 0.01	6.93 ± 0.04	7.70 ± 0.14
	0.93 ± 0.03	1.01 ± 0.06	0.95 ± 0.03	0.89 ± 0.10	0.94 ± 0.02
Secoverine	8.85 ± 0.02	8.86 ± 0.05	8.28 ± 0.04	9.44 ± 0.05	9.31 ± 0.02
	1.05 ± 0.05	1.09 ± 0.09	0.97 ± 0.03	1.07 ± 0.03	1.04 ± 0.03
Tropicamide	7.18 ± 0.04	7.30 ± 0.05	7.42 ± 0.05	7.17 ± 0.04	7.85 ± 0.07
	0.88 ± 0.04	0.97 ± 0.06	0.96 ± 0.02	1.05 ± 0.02	0.94 ± 0.01
Aprophen	9.07 ± 0.01	8.31 ± 0.07	8.47 ± 0.09	8.26 ± 0.03	8.42 ± 0.09
	1.09 ± 0.15	0.94 ± 0.04	0.91 ± 0.09	0.96 ± 0.02	0.96 ± 0.04
Atropine	9.55 ± 0.10	9.01 ± 0.04	9.51 ± 0.06	9.15 ± 0.07	9.56 ± 0.09
	1.04 ± 0.06	1.04 ± 0.02	0.95 ± 0.04	0.97 ± 0.03	1.07 ± 0.03
Benzhexol	9.13 ± 0.14	7.86 ± 0.05	8.53 ± 0.06	8.71 ± 0.04	8.71 ± 0.07
	0.95 ± 0.11	0.94 ± 0.02	0.92 ± 0.05	1.02 ± 0.03	0.89 ± 0.04
Benztropine	9.60 ± 0.01[a]	8.42 ± 0.00	9.15 ± 0.11	8.68 ± 0.07	9.05 ± 0.04
	1.03 ± 0.08	1.19 ± 0.07	1.02 ± 0.11	1.07 ± 0.06	1.05 ± 0.10
Biperiden	9.27 ± 0.06	7.97 ± 0.08	8.73 ± 0.11	8.77 ± 0.08	8.69 ± 0.10
	1.08 ± 0.00	1.00 ± 0.02	0.89 ± 0.08	0.96 ± 0.03	0.92 ± 0.02
Botiacrine	8.52 ± 0.04	7.97 ± 0.02	7.78 ± 0.09	8.37 ± 0.07	8.29 ± 0.10
	0.96 ± 0.04	0.90 ± 0.06	0.88 ± 0.04	1.03 ± 0.02	0.91 ± 0.05
BTM1086	9.54 ± 0.11[a]	8.31 ± 0.04	9.06 ± 0.05[a]	8.69 ± 0.02	9.00 ± 0.04
	1.18 ± 0.13	0.97 ± 0.04	0.96 ± 0.04	0.98 ± 0.02	0.99 ± 0.03
CCI19234	8.89 ± 0.04	7.47 ± 0.04	8.01 ± 0.09	8.48 ± 0.11	8.41 ± 0.05[a]
	1.18 ± 0.03	0.88 ± 0.05	0.96 ± 0.04	1.03 ± 0.01	1.02 ± 0.11
Cyclopentolate	8.79 ± 0.02	7.56 ± 0.01	8.58 ± 0.01	8.33 ± 0.05[a]	8.59 ± 0.04[a]
	0.94 ± 0.02	0.96 ± 0.03	0.96 ± 0.01	1.00 ± 0.03	0.93 ± 0.12
4-DAMP	8.99 ± 0.16	8.15 ± 0.03	9.23 ± 0.06	8.32 ± 0.07	8.85 ± 0.06
	0.82 ± 0.03	1.02 ± 0.02	0.97 ± 0.06	1.05 ± 0.05	0.95 ± 0.03
Dicyclomine	9.21 ± 0.07	7.49 ± 0.04	8.75 ± 0.05	8.26 ± 0.15	8.82 ± 0.11
	1.08 ± 0.07	0.94 ± 0.05	0.97 ± 0.02	1.05 ± 0.02	0.90 ± 0.06
Eucatropine	7.04 ± 0.02	6.49 ± 0.02	6.36 ± 0.05	6.37 ± 0.09	6.67 ± 0.09
	0.95 ± 0.02	1.00 ± 0.04	0.93 ± 0.01	0.98 ± 0.03	1.02 ± 0.02
HSD	8.14 ± 0.05	6.92 ± 0.04	8.40 ± 0.03	7.61 ± 0.01	7.97 ± 0.05
	1.04 ± 0.07	0.95 ± 0.02	0.96 ± 0.03	1.03 ± 0.01	0.88 ± 0.04
Homatropine	7.38 ± 0.04	6.78 ± 0.04	7.23 ± 0.03	7.14 ± 0.05	7.60 ± 0.01
	0.98 ± 0.01	0.89 ± 0.02	0.94 ± 0.04	1.00 ± 0.04	0.94 ± 0.02
Ipratropium	9.15 ± 0.07	9.44 ± 0.02	9.43 ± 0.04	9.67 ± 0.09	9.89 ± 0.10
	0.83 ± 0.05	0.94 ± 0.02	0.95 ± 0.05	0.98 ± 0.01	0.98 ± 0.04
Orphenadrine	7.39 ± 0.02	6.85 ± 0.02	7.01 ± 0.08	6.67 ± 0.09	7.09 ± 0.10
	0.94 ± 0.04	0.95 ± 0.04	0.95 ± 0.00	0.97 ± 0.01	0.96 ± 0.04
Oxybutinin	9.19 ± 0.04	8.50 ± 0.05	9.20 ± 0.07	8.57 ± 0.04	9.35 ± 0.06
	1.14 ± 0.10	0.92 ± 0.02	1.03 ± 0.08	1.02 ± 0.04	0.92 ± 0.04
Piperidolate	7.19 ± 0.04	6.85 ± 0.04	6.81 ± 0.02	7.44 ± 0.03	7.19 ± 0.01
	0.97 ± 0.03	0.95 ± 0.04	0.96 ± 0.02	1.02 ± 0.03	0.95 ± 0.01
Procyclidine	8.35 ± 0.06	7.37 ± 0.03	8.14 ± 0.06	8.22 ± 0.08	8.32 ± 0.11
	1.05 ± 0.04	0.94 ± 0.03	0.97 ± 0.01	0.93 ± 0.04	0.95 ± 0.01
PrBCh	8.15 ± 0.07[a]	8.38 ± 0.14	8.09 ± 0.14	8.63 ± 0.04	8.23 ± 0.05
	0.88 ± 0.07	0.98 ± 0.06	1.02 ± 0.03	1.01 ± 0.01	1.03 ± 0.05
Scopolamine	9.73 ± 0.05[a]	8.85 ± 0.02[a]	9.74 ± 0.02[a]	9.03 ± 0.07	9.65 ± 0.02
	1.08 ± 0.06	0.87 ± 0.06	1.01 ± 0.01	1.00 ± 0.02	0.94 ± 0.04
Telenzepine	8.89 ± 0.05	7.77 ± 0.00	8.12 ± 0.09	8.61 ± 0.05	8.58 ± 0.09
	1.21 ± 0.14	0.97 ± 0.01	1.00 ± 0.01	1.04 ± 0.05	0.95 ± 0.03

[a] Mean and range/2 of two experiments; all other results are mean and standard error of $n \geq 3$ experiments.

Kinetic studies. Kinetic parameters for [^{3}H]NMS and [^{3}H]PRZ are shown in Table 2. [^{3}H]PRZ dissociated relatively slowly in all tissues studied, and dissociation was slower in rabbit cortex than in rat cortex. Dissociation rates in rabbit lung and chicken heart were similar to each other and more rapid than in cortex. At radioligand concentrations less than the K_d such as those practically feasible with [^{3}H]PRZ, the observed association rate constant, K_{obs}, approximates the dissociation rate constant, so no attempt was made to measure the true association rate constants for [^{3}H]PRZ.

The dissociation rate constants for [^{3}H]NMS roughly paralleled its K_d values in the tissues studied, with $t_{1/2}$ values ranging from 2.5 min in rat heart to 43 min in rat gland. The dissociation rate in rabbit lung was one third the rate in chicken heart

TABLE 4

Selectivity of antagonists at five muscarinic binding sites

The antagonists' selectivity at each pair of sites is the ratio of the larger K_i to the smaller; where the first K_i in the comparison is the larger (i.e., the antagonist has lower affinity at the first site), the ratio is preceded by a minus sign. The sites are [^{3}H]PRZ in the rat cortex (M_1), [^{3}H]NMS in rat heart (M_2), [^{3}H]NMS in rat submandibular gland (M_3), [^{3}H]NMS in chicken heart (CH), and [^{3}H]NMS in rabbit peripheral lung (RL). The K_i or [^{3}H]NMS K_d values are derived from Tables 1 and 3.

Drug	Selectivity ratio									
	RL vs. M_1	RL vs. M_2	RL vs. M_3	RL vs. CH	CH vs. M_1	CH vs. M_2	CH vs. M_3	M_1 vs. M_2	M_1 vs. M_3	M_2 vs. M_3
[^{3}H]NMS		4	1	3		1	−3			−3
PRZ	−4	10	2	−1	−3	13	3	35	9	−4
Himbacine	11	−1	13	1	11	−1	13	−15	1	18
Methoctramine	2	−3	9	−1	2	−3	10	−5	5	29
DABDMA	−1	11	−2	6	−9	2	−12	17	−1	−22
Secoverine	3	3	11	−1	4	4	14	−1	4	4
Tropicamide	5	4	3	5	−1	−1	−2	−1	−2	−1
Aprophen	−4	1	−1	1	−6	−1	−2	6	4	−1
Atropine	1	4	1	3	−3	1	−2	3	1	−3
Benzhexol	−3	7	2	0	−3	7	2	19	4	−5
Benztropine	−4	4	−1	2	−8	2	−3	15	3	−5
Biperiden	−4	5	−1	−1	−3	6	1	20	3	−6
Botiacrine	−2	2	3	−1	−1	3	4	4	5	2
BTM1086	−3	5	−1	2	−7	2	−2	17	3	−6
CCI19234	−3	9	3	−1	−3	10	3	26	8	−3
Cyclopentolate	−2	11	1	2	−3	6	−2	17	2	−10
4-DAMP	−1	5	−2	3	−5	1	−8	7	−2	−12
Dicyclomine	−2	21	1	4	−9	6	−3	52	3	−18
Eucatropine	−2	2	2	2	−5	−1	1	4	5	1
HSD	−1	11	−3	2	−3	5	−6	17	−2	−30
Homatropine	2	7	2	3	−2	2	−1	4	1	−3
Ipratropium	5	3	3	2	3	2	2	−2	−2	1
Orphenadrine	−2	2	1	3	−5	−2	−2	3	2	−1
Oxybutinin	1	7	1	6	−4	1	−4	5	−1	−5
Piperidolate	0	2	2	−2	2	4	4	2	2	1
Procyclidine	−1	9	2	1	−1	7	1	10	2	−6
PrBCh	1	−1	1	−3	3	2	3	−2	1	2
Scopolamine	−1	6	−1	4	−5	2	−5	8	−1	−8
Telenzepine	−2	6	3	−1	−2	7	3	13	6	−2

and twice the rate in NG108-15 cells (Fig. 2). The [^{3}H]NMS dissociation rate of each tissue was significantly different from that of every other tissue ($p < 0.05$). The kinetically derived K_d estimates are in good agreement with those derived from saturation analysis, except for rat and chicken heart, in which the association rate constant estimates were probably inacurate because the radioligand concentration was similar to the K_d and, therefore, too low for accurate estimates.

The dissociation of [^{3}H]NMS from NG108-15 membranes appeared to contain a rapid component (Fig. 2), and these curves were analyzed further with a nonlinear procedure. A two-component model provided a much better fit than a one-component model ($p < 0.05$ to $p < 0.001$, $K_1 = 0.46 \pm 0.13$ min^{-1}, $K_2 = 0.021 \pm 0.001$ min^{-1}, $n = 3$), with the fast component comprising 21 ± 5% of the bound sites.

Agonist inhibition studies. The ability of magnesium and a guanine nucleotide to modulate agonist binding to chicken heart and rabbit lung is shown in Fig. 3. In the absence of magnesium, Gpp(NH)p increased the slope and IC_{50} for carbachol in chicken heart but had no effect in rabbit lung. Magnesium alone decreased the slope and IC_{50} for carbachol in both tissues, and the addition of Gpp(NH)p increased the slope and IC_{50} to the values observed with Gpp(NH)p alone. Magnesium and Gpp(NH)p had no effect on [^{3}H]NMS saturation parameters (data not shown).

Antagonist inhibition studies. [^{3}H]PRZ binding in chicken heart and rabbit lung was inhibited by himbacine and PRZ with pK_i values very similar to those found when [^{3}H]NMS was used as the label. PRZ had pK_i values very similar to the pK_d values measured in saturation studies and was about 3-fold weaker against [^{3}H]PRZ in chicken heart and rabbit lung than in rabbit cortex (pK_i, 7.4, 7.6, and 8.1, respectively). Himbacine, in contrast, inhibited [^{3}H]PRZ binding with 10-fold greater potency in chicken heart and rabbit lung than in rat cortex (Fig. 4) (pK_i in chicken heart, 8.1 ± 0.1, $n = 2$; rabbit lung, 8.1 ± 0.1, $n = 2$; rat cortex, 7.1). Himbacine had a similar pK_i at [^{3}H]PRZ sites in rabbit cortex (7.1) and in rat cortex.

The pK_i and slope values for a number of antagonists against [^{3}H]PRZ in rat cortex and [^{3}H]NMS in rat heart, rat gland, chicken heart, and rabbit lung are shown in Table 3. In rabbit lung, most drugs had slope factors of about unity, but himbacine and methoctramine had somewhat shallow slopes, suggesting that rabbit lung may contain a small component of M_3 sites. All compounds had slopes of about unity in chicken heart. Table 4 shows the ratio of K_i values for each drug at each pair of sites. Most compounds did not differentiate between the various sites, but a number of compounds showed about 10-fold selectivity between the sites in rabbit lung and at least one of the other sites. Himbacine was weaker at M_1 sites, and PRZ and DABDMA were weaker at M_2 sites, as were cyclopentolate, dicyclomine, HSD, and procyclidine; himbacine, methoctramine, and secoverine were weaker at M_3 sites. Few compounds distinguished between chicken heart and rabbit lung, but DABDMA, tropicamide, and oxybutinin were about 5-fold more potent in rabbit lung. Fig. 5 shows occupancy curves for secoverine and tropicamide in the five tissues. Fig. 6 shows the pK_i

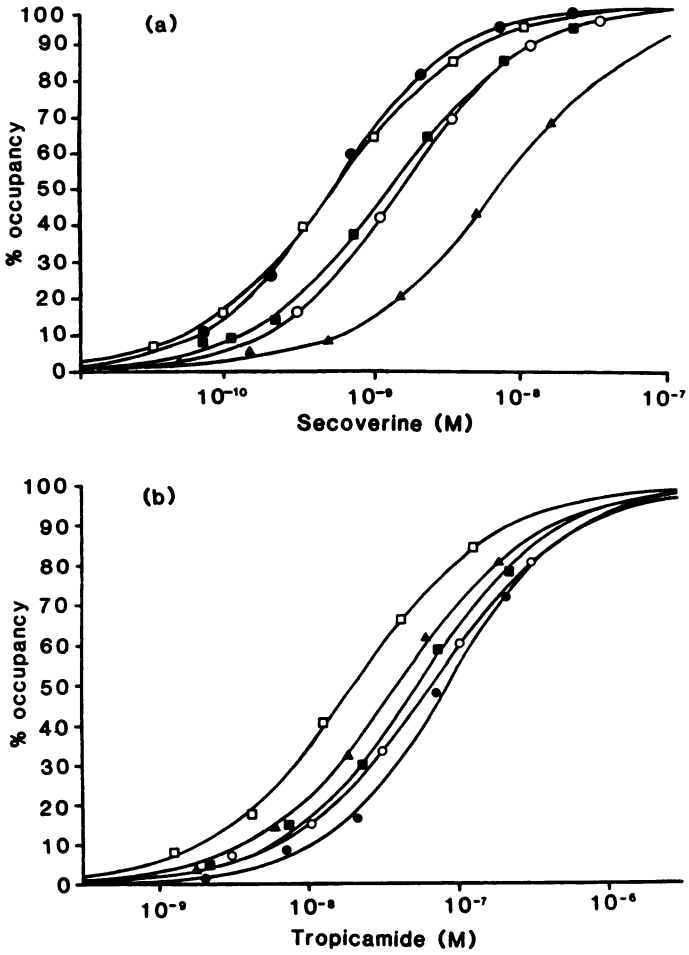

Fig. 5. Occupancy curves of secoverine and tropicamide in five tissues. Membranes from rat cortex were incubated with 0.6 nM [^{3}H]PRZ (M_1 sites) (○), and membranes from rat heart (M_2 sites) (■), rat gland (M_3 sites) (▲), chicken heart (●), and rabbit lung (□) were incubated with 0.1 nM [^{3}H]NMS in the presence of various concentrations of secoverine (a) or topicamide (b). Nonspecific binding was measured in the presence of 1 μM atropine. The influence of the fixed [^{3}H]NMS concentration has been accounted for by adjusting the antagonist concentrations used with a particular tissue according to the equation $[A'] = [A]/([L]/K_d + 1)$, where $[A]$ is the actual concentration of antagonist, $[L]$ is the fixed concentration of [^{3}H]NMS, K_d is the K_d of [^{3}H]NMS in the tissue, and $[A']$ is the adjusted antagonist concentration plotted in the graphs. The data for each antagonist were obtained in a single experiment conducted in duplicate.

values of six of the most discriminating compounds, PRZ, himbacine, methoctramine, DABDMA, secoverine, and tropicamide, at the non-lung sites, compared with their pK_i values at rabbit lung sites. It is apparent that rabbit lung is more similar to chicken heart than to any other site.

In a further series of experiments, this set of six discriminating compounds was studied in parallel in rabbit lung and NG108-15 cell membranes (Table 5, Fig. 7). The [^{3}H]NMS sites in rabbit lung were almost identical to those in NG108-15 cells, although the 2-fold lower affinity of PRZ for NG108-15 sites precludes the use of [^{3}H]PRZ to label and characterize these sites.

Northern blots. Results of Northern blot analysis are shown in Fig. 8. A single 3-kb hybridizing transcript was detected with the m4 oligonucleotide probes, whereas no signal was seen with m1, m2, m3, or m5 probes.

Discussion

The first subdivision of muscarinic receptors based on a selective competitive antagonist was made by Barlow *et al.* (22), who described the functional selectivity of 4-DAMP for smooth muscle compared with cardiac muscarinic receptors. The subsequent development of the selective antagonists PRZ (23), HSD (24), AF-DX116 (25), himbacine (26), and methoctramine (27) has led to the subdivision of muscarinic receptors into M_1, M_2 (cardiac), and M_3 (glandular or functional smooth muscle) subtypes (28). Molecular biological studies have identified the genes that probably generate these muscarinic receptor subtypes, the m1, m2, and m3 genes (28). It is known, however, that at least two other types of muscarinic receptor gene, the m4 and m5 genes, are expressed in mammalian tissue (1–4), and a number of muscarinic receptors, characterized pharmacologically in functional or binding studies, do not fit readily into the M_1, M_2, and M_3 pharmacological classification. The binding sites in chicken heart and rabbit lung are two such atypical muscarinic receptors, and here we have attempted to establish pharmacological criteria for determining whether one or both of these sites represent the M_4 site. Using these criteria, we found a close similarity between rabbit lung sites and putative m4 sites in NG108-15 cells, and we have supported the validity of the pharmacology by demonstrating a predominance of m4 mRNA in rabbit lung.

Muscarinic receptors in chick heart are similar to mammalian heart (M_2) receptors in supporting high affinity guanine nucleotide-sensitive agonist binding (Ref. 29 and this study) and mediating inhibition of adenylyl cyclase (12), but unlike mammalian M_2 receptors they have high affinity for PRZ (Ref. 12 and this study). They mediate a negative inotropic response (30, 31) and inhibition of acetylcholine release (30). Choo *et al.* (31) measured the pA_2 or pK_b values of a number of antagonists for inhibition of the negative inotropic effect in chick atria. Their values for secoverine, PRZ, and 4-DAMP were similar to our binding values in chicken heart, but their values for atropine, himbacine, and methoctramine were about 10-fold lower than ours. Our results are very similar to comparable binding values reported recently (32).

There are species differences in the muscarinic binding characteristics of mammalian lung parenchyma. PRZ has moderate to low potency in rat and guinea pig lung and higher potency in rabbit and human lung (Ref. 33–37 and this study). The sites in rabbit lung can be distinguished from those in human lung and from M_1 sites by their higher affinity for AF-DX116 (13, 34, 37) and himbacine (this study),[3] although the heterogeneity of sites in human lung precludes firm conclusions at this time about their subtype composition. The location of the binding sites within rabbit lung parenchyma is unknown but they may not be on smooth muscle, because Bloom *et al.* (38) found that PRZ had low affinity for agonist-contracted rabbit bronchial rings. These authors also found that PRZ had high potency in blocking vagally induced bronchoconstriction in the rabbit, but this is disputed (39).

All the antagonists that we studied had relatively high affinity for rabbit lung, including those considered to be M_1 selective (PRZ and telenzepine), M_2 selective (himbacine and methoctramine), and M_3 selective (HSD, 4-DAMP, and DABDMA). Bloom *et al.* (33) found shallow slopes with PRZ in competition

[3] S. Lazareno, unpublished observations.

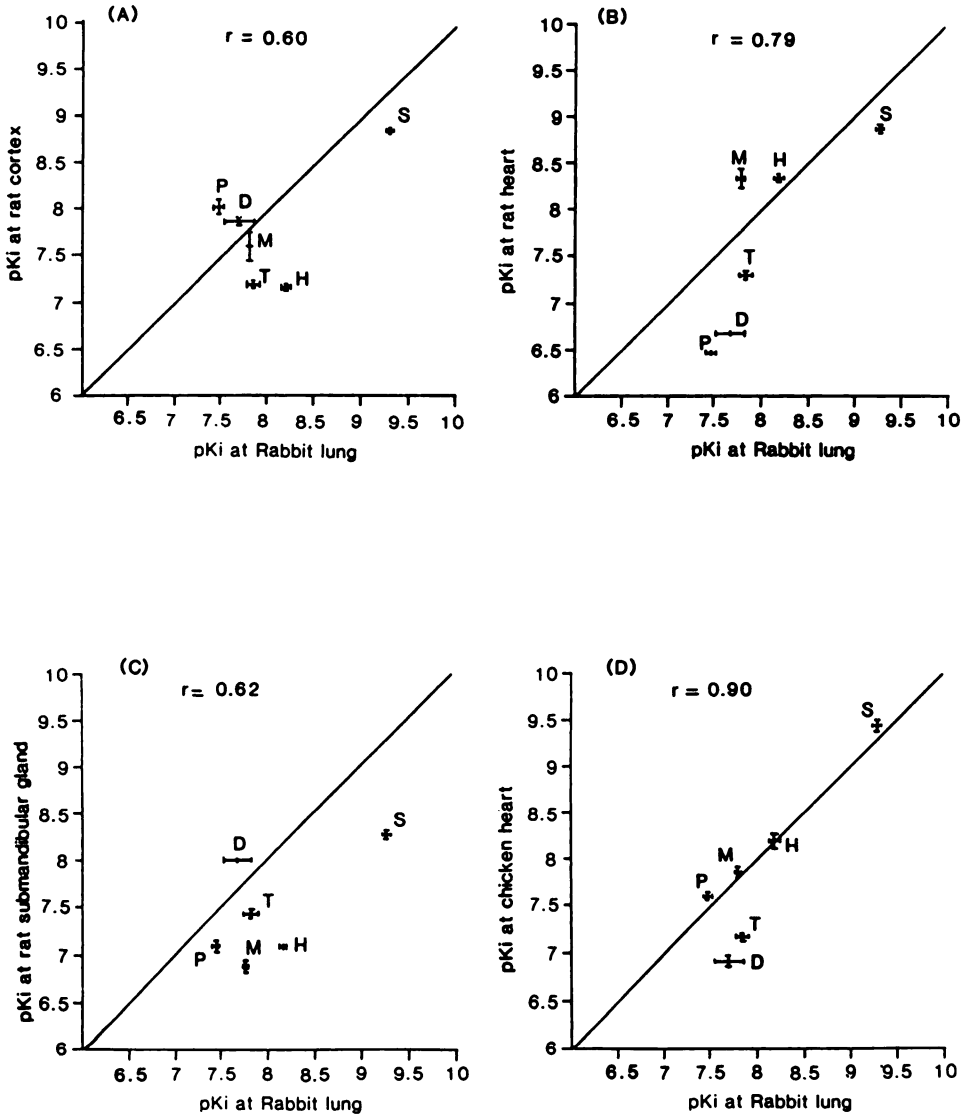

Fig. 6. Comparison between pK_i values of PRZ (*P*), himbacine (*H*), methoctramine (*M*), DABDMA (*D*), secoverine (*S*), and tropicamide (*T*) at [^{3}H]NMS sites in rabbit lung and their pK_i values at [^{3}H]PRZ sites in rat cortex (M_1) (A) and [^{3}H]NMS sites in rat heart (M_2) (B), rat submandibular gland (M_3) (C), and chicken heart (D). The two standard errors on each point are shown. The data are from Table 3.

TABLE 5

pK_i values of selective antagonists in rabbit lung and NG108-15 cell membranes

Each experiment contained a saturation curve for [^{3}H]NMS and inhibition curves for five antagonists in the presence of 0.1 nM [^{3}H]NMS in both rabbit lung and NG108-15 membranes. The saturation curves were analyzed by the program LIGAND according to a one-site model. Inhibition curves were analyzed with the program ALLFIT and IC_{50} values were converted to K_i values using the [^{3}H]NMS K_d measured in the same experiment and the equation of Cheng and Prusoff (20). The K_d (pM) and B_{max} (fmol/mg of protein) were, respectively, rabbit lung, 34 ± 3 and 184 ± 3; NG108-15 cells, 25 ± 2 and 105 ± 14; n = 4).

	n	Rabbit lung		NG108-15	
		pK_i	Slope	pK_i	Slope
PRZ	3	7.55 ± 0.05	0.97 ± 0.03	7.20 ± 0.05	0.93 ± 0.01
Himbacine	3	8.47 ± 0.05	0.85 ± 0.02	8.53 ± 0.02	0.92 ± 0.03
Methoctramine	4	7.83 ± 0.11	0.82 ± 0.01	8.09 ± 0.07	0.78 ± 0.05
DABDMA	3	7.58 ± 0.09	1.00 ± 0.10	7.71 ± 0.03	1.00 ± 0.04
Secoverine	3	9.48 ± 0.03	1.03 ± 0.06	9.28 ± 0.03	1.06 ± 0.06
Tropicamide	2	8.00 ± 0.05	0.97 ± 0.01	8.08 ± 0.03	0.99 ± 0.02

with [^{3}H]quinuclidinyl benzilate, and they concluded that high affinity [^{3}H]PRZ sites comprised about 80% of the total muscarinic population. In our studies, PRZ gave slope values approaching unity, and a possible contribution of M_3 sites to the slightly shallow slopes observed with himbacine and methoctramine was too small to quantify accurately. It is thought that highly lipophilic radioligands such as [^{3}H]quinuclidinyl benzilate can label a population of sites in membranes to which less lipophilic ligands such as PRZ and [^{3}H]NMS have limited access (40), and this may have contributed to the small PRZ slopes observed by Bloom *et al.* (33). The second messenger coupling of muscarinic receptors in rabbit lung parenchyma has not, to our knowledge, been reported, but, in contrast to Bloom *et al.* (33), we found that agonist binding to these sites was modified by guanine nucleotides.

There are three previous reports on selective antagonist binding to NG108-15 cells. One study (41) found a portion of the sites to bind [^{3}H]PRZ with high affinity, whereas our results agree with those of the others (42, 43) in finding that the pK_i of PRZ of about 7.2 was too low to allow readily detectable [^{3}H]PRZ binding. We found no evidence for a small population of high affinity PRZ sites, either in displacement studies or in direct binding studies with [^{3}H]PRZ. With regard to other antagonists, the values reported by Michel *et al.* (43) in NG108-15 membranes for PRZ, methoctramine, and 4-DAMP are virtually identical to the values we obtained in NG108-15 and/or rabbit lung membranes. Our values differ considerably, how-

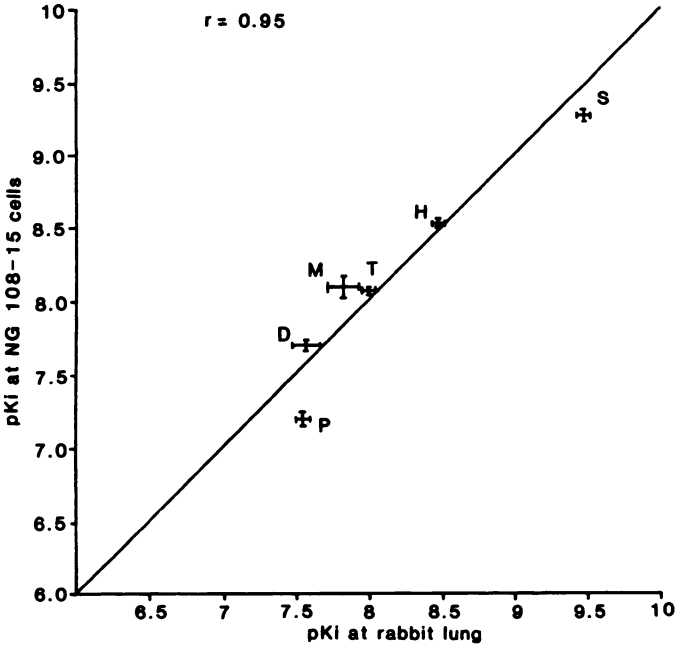

Fig. 7. Comparison between pK_i values of PRZ (*P*), himbacine (*H*), methoctramine (*M*), DABDMA (*D*), secoverine (*S*), and tropicamide (*T*) at [^{3}H]NMS sites in membranes from NG108-15 cells and rabbit lung. The two standard errors on each point are shown. The data are from Table 5.

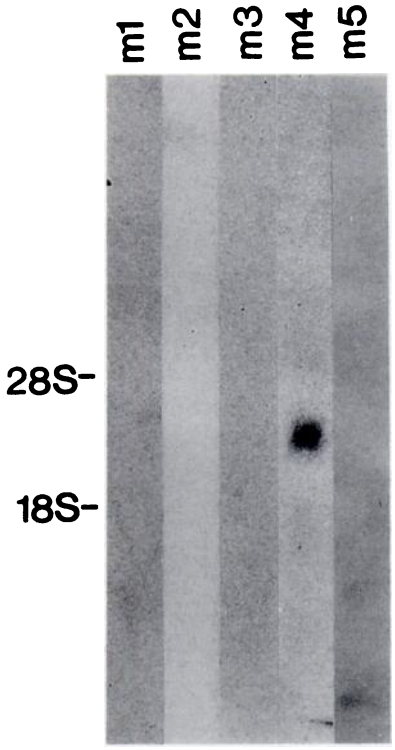

Fig. 8. Northern blot analysis of total cellular rabbit lung RNA. Size markers are provided by the 28 S and 18 S ribosomal bands corresponding to 5.1 and 2.0 kb, respectively. Approximate size of the hybridizing m4 transcript is 3 kb.

ever, from values observed by Michel *et al.* (44) at M_1, M_2, M_3, and PC12 cell sites, although the latter cells were reported to have an identical pharmacology to NG108-15 cells (43). This discrepancy could be accounted for by the different buffers used in the two studies of Michel *et al.*[4] Our results in NG108-15 cells are also consistent with results in m4-transfected cells (9, 10).

NG108-15 cells have been reported to express only m4 RNA (2).[5] In kinetic experiments with these cells, however, we found a rapidly dissociating component of [^{3}H]NMS binding. We also found that displacement curves with methoctramine in these cells had shallow slopes, and there was a (nonsignificant) trend for higher pK_i values to correlate with lower slopes ($r = 0.7$, $n = 5$). Although shallow slopes may relate to an allosteric effect observed with methoctramine at concentrations above 1 μM (45, 46),[6] this pattern of results is also consistent with the presence of a population of M_2 sites together with M_4 sites in our NG108-15 cells. The finding that methoctramine was the only compound to give flat slopes in NG108-15 cells may be explained by the fact that methoctramine was the only compound to have higher potency at M_2 (rat heart) sites than at NG108-15 sites, and its ability to discriminate an M_2 component among the NG108-15 sites would be enhanced by the opposite selectivity of the radioligand [^{3}H]NMS (8).

In general, our results at M_1, M_2, and M_3 sites confirm and extend those reported previously (7, 8, 47–50) but the data for two compounds require comment. (a) Although we agree with Takayanagi *et al.* (51) that BTM1086 distinguishes between M_1 and M_2 sites, we did not find it to be selective between M_1 and M_3 sites. (b) DABDMA was reported (52) to be the most selective of a series of tertiary 4-DAMP analogues in functional studies with guinea pig ileum and atria. Among the drugs we have tested, it was second only to HSD in its selectivity for M_3 and M_2 sites. Like HSD and 4-DAMP, however, it did not distinguish between M_1 and M_4 sites.

The binding sites in rabbit lung do not fall into the M_1–M_3 category. They cannot be M_1 sites because himbacine had 10-fold higher affinity at these sites than at 'true' M_1 sites in rat cortex, and this is not merely a species difference, because himbacine had a similar low affinity at M_1 sites in rabbit and rat cortex. Rabbit lung sites cannot be M_2 sites because of their relatively high affinity for PRZ, cyclopentolate, and dicyclomine, and they cannot be M_3 sites because of their high affinity for himbacine, methoctramine, and secoverine.

The sites in chicken heart are pharmacologically similar to those in rabbit lung, with high affinity for PRZ, himbacine, and secoverine, the latter compound with overall selectivity for these tissues, but they are not identical because DABDMA and [^{3}H]NMS are 3–6-fold more potent in rabbit lung. Tropicamide and oxybutinin are also about 5-fold more potent in rabbit lung than in chicken heart, the former compound with an overall 3–5-fold selectivity for rabbit lung. Chick and mammalian heart receptors have different structures (29) and the chick heart receptor has recently been cloned and sequenced (53). Interestingly, it has the greatest homology with the mammalian m4 receptor and has, therefore, been designated the cm4 receptor. This structural similarity between m4 and cm4 receptors is consistent with the pharmacological similarity we found between rabbit lung and chicken heart sites. The cm4 receptor may also occur in avian brain (53, 54).

Having assessed a range of antagonists in the five tissues, we chose six of the most discriminating compounds to compare

[4] A. Michel, personal communication.
[5] N. Buckley, unpublished observations.
[6] S. Lazareno, unpublished observations.

the muscarinic sites in rabbit lung and NG108-15 cell membranes. NG108-15 cells have been reported to express exclusively the m4 receptor (2), so this was a pharmacological test of the hypothesis that the rabbit lung contains M_4 sites. We found that rabbit lung was more similar to NG108-15 cells than to any other tissue studied. The largest discrepancy was that PRZ was 2-fold less potent in NG108-15 cells, and this difference spanned a practical threshold allowing reasonable [^{3}H] PRZ specific binding only to rabbit lung. Overall, however, the two sites were very similar; the pK_i values of the six compounds in the two tissues were highly correlated (r = 0.95) and the regression line had a slope not significantly different from unity and an intercept not significantly different from zero.

Dissociation kinetics provide another criterion for distinguishing among receptor subtypes (55). Our values for [^{3}H] NMS dissociation rate are very similar to other reports (32, 43), and each tissue in our study had a significantly different value from every other tissue. The 8–17-fold difference between rat gland and chicken or rat heart clearly supports the conclusion that these are different subtypes, and the 3-fold difference between chicken heart and rabbit lung may support the same conclusion. The [^{3}H]NMS dissociation rate constants for gland, rabbit lung, and NG108-15 cells, however, differed by only about 2-fold or less, as did the [^{3}H]PRZ dissociation rates in cortex and lung. These differences are probably too small to contribute to the identification of receptor subtypes.

The close pharmacological similarity between muscarinic sites in rabbit lung and NG108-15 cells led us to study the muscarinic receptor mRNA in rabbit lung. The predominance of m4 transcripts in this tissue supports the notion that the rabbit lung muscarinic site characterized in the present study corresponds to an m4 muscarinic receptor. This is the first time that mammalian m4 mRNA has been localized to nonneural tissue. Previously, m4 transcripts have been found only in specific brain regions (56), autonomic ganglia,[7] and neural cell lines. Further studies are required to identify the cell types in rabbit lung that express the m4 receptor and to determine whether the small pharmacological differences between rabbit lung and NG108-15 sites relate to species differences, differences in membrane environment, or some other factor.

In conclusion, rabbit peripheral lung contains muscarinic binding sites characterized by a moderate to high affinity for PRZ, himbacine, and secoverine. They are pharmacologically distinct from M_1, M_2, or M_3 sites, are more similar to muscarinic sites in chicken heart, and are most similar to muscarinic sites in NG108-15 cells. These results, and the presence of muscarinic m4 receptor mRNA, suggest that rabbit lung contains muscarinic sites of the M_4 subtype.

Acknowledgments

We are grateful to Dr. E. Kawashima for his support and the supply of oligonucleotides, Dr. G. McDowell for culturing the cells, and Mr. J. Brown for technical assistance.

References

1. Bonner, T. I., N. J. Buckley, A. C. Young, and M. R. Brann. Identification of a family of muscarinic acetylcholine receptor genes. *Science (Washington D. C.)* **237**:527–533 (1987).
2. Peralta, E. G., A. Ashkenazi, J. W. Winslow, D. H. Smith, J. Ramachandran, and D. J. Capon. Distinct primary structures, ligand-binding properties and tissue specific expression of four human muscarinic acetylcholine receptors. *EMBO J.* **6**:3923–3929 (1987).
3. Bonner, T. I., A. C. Young, M. R. Brann, and N. J. Buckley. Cloning and expression of the human and rat m5 muscarinic acetylcholine receptor genes. *Neuron* **1**:403–410 (1988).
4. Liao, C.-F., A. P. N. Themmen, R. Joho, C. Barberis, M. Birnbaumer, and L. Birnbaumer. Molecular cloning and expression of a fifth muscarinic acetylcholine receptor. *J. Biol. Chem.* **264**:7328–7337 (1989).
5. Maeda, A., T. Kubo, M. Mishina, and S. Numa. Tissue distribution of mRNAs encoding muscarinic aceylcholine receptor subtypes. *FEBS Lett.* **239**:339–342 (1988).
6. Bonner, T. I. The molecular basis of muscarinic receptor diversity. *Trends Neurosci.* **12**:148–151 (1989).
7. Doods, H. N., M. J. Mathy, D. Davidesko, K. J. Van Charldorp, A. De Jonge, and P. A. Van Zwieten. Selectivity for muscarinic antagonist in radioligand and *in vivo* experiments for the putative M_1, M_2 and M_3 receptors. *J. Pharmacol. Exp. Ther. 242*:257–263 (1987).
8. Lazareno, S., and F. F. Roberts. Functional and binding studies with muscarinic M_2-subtype selective antagonists. *Br. J. Pharmacol.* **98**:309–317 (1989).
9. Akiba, I., T. Kubo, A. Maeda, H. Bujo, J. Nakai, M. Mishina, and S. Numa. Primary structure of porcine muscarinic acetylcholine receptor III and antagonist binding studies. *FEBS Lett.* **235**:257–261 (1988).
10. Buckley, N. J., T. I. Bonner, C. M. Buckley, and M. R. Brann. Antagonist binding properties of five cloned muscarinic receptors expressed in CHO-K1 cells. *Mol. Pharmacol.* **35**:469–476 (1989).
11. Peralta, E. G., A. Ashkenazi, J. W. Winslow, J. Ramachandran, and D. J. Capon. Differential regulation of PI hydrolysis and adenylyl cyclase by muscarinic receptor subtypes. *Nature (Lond.)* **334**:434–437 (1988).
12. Brown, J. H., D. Goldstein, and S. B. Masters. The putative M_1 muscarinic receptor does not regulate phosphoinositide hydrolysis: studies with pirenzepine and McNA-343 in chick heart and astrocytoma cells. *Mol. Pharmacol.* **27**:525–531 (1985).
13. Bloom, J. W., M. Halonen, N. A. Seaver, and H. I. Yamamura. Heterogeneity of the M_1 muscarinic receptor subtype between peripheral lung and cerebral cortex demonstrated by the selective antagonist AF-DX 116. *Life Sci.* **41**:491–496 (1987).
14. Hamprecht, B. Structural, electrophysiological, biochemical, and pharmacological properties of neuroblastoma-glioma cell hybrids in cell culture. *Int. Rev. Cytol.* **49**:99–170 (1977).
15. Ensing, K., D. A. Bloemhof, W. G. Hout, and R. A. De Zeeuw. Discrepancies in the specific activity of ^{3}H-*N*-methylscopolamine as determined by mass spectrometry and radioreceptor assay due to racemisation. *J. Receptor Res.* **8**:871–883 (1988).
16. Chomczynski, P., and N. Sacchi. Single-step method of RNA isolation by acid guanidinium thiocyanate-phenol-chloroform extraction. *Anal. Biochem.* **162**:156–159 (1987).
17. Gocayne, J., D. A. Robinson, M. G. Fitzgerald, F.-Z. Chung, A. R. Kerlavage, K.-U. Lentes, J. Lai, C.-D. Wang, C. M. Fraser, and J. C. Venter. Primary structure of rat cardiac β-adrenergic and muscarinic cholinergic receptors obtained by automated DNA sequence analysis: further evidence for a multigene family. *Proc. Natl. Acad. Sci. USA* **84**:8296–8300 (1987).
18. Munson, P. J., and D. Rodbard. LIGAND: a versatile computerized approach for characterization of lingand-binding systems. *Anal. Biochem.* **107**:220–239 (1980).
19. DeLean, A., P. J. Munson, and D. Rodbard. Simultaneous analysis of families of sigmoidal curves: application to bioassay, radioligand assay and physiological dose-response curves. Am. J. Physiol. **235**:E97–E102 (1978).
20. Cheng, Y., and W. H. Prusoff. Relationship between the inhibition constant (K_i) and the concentration of inhibitor which caused 50 per cent inhibition (I_{50}) of an enzymatic reaction. *Biochem. Pharmacol.* **22**:3099–3108 (1973).
21. Eberlein, W. G., G. Trummlitz, W. W. Engle, G. Schmidt, H. Pelzer, and N. Mayer. Tricyclic compounds as selective antimuscarinics. 1. Structural requirements for selectivity toward the muscarinic acetylcholine receptor in a series of pirenzepine and imipramine analogues. *J. Med. Chem.* **30**:1378–1382 (1987).
22. Barlow, R. D., K. J. Berry, P. A. M. Glenton, N. M. Nikolaou, and K. S. Soh. A comparison of affinity constants for muscarine-sensitive acetylcholine receptors in guinea-pig atrial pacemaker cells at 29°C and in ileum at 29°C and 37°C. *Br. J. Pharmacol.* **58**:613–620 (1976).
23. Hammer, R., C. P. Berrie, N. J. M. Birdsall, A. S. V. Burgen, and E. C. Hulme. Pirenzepine distinguishes between different subclasses of muscarinic receptors. *Nature (Lond.)* **283**:90–92 (1980).
24. Mutschler, E., and G. Lambrecht. Selective muscarinic agonists and antagonists in functional tests. *Trends Pharmacol. Sci.* **5**(suppl.):39–44 (1984).
25. Giachetti, A., R. Micheletti, and E. Montagna. Cardioselective profile of AF-DX 116, a muscarine M_2 receptor antagonist. *Life. Sci.* **38**:1663–1672 (1986).
26. Gilani, A. S. H., and L. B. Cobbin. The cardio-selectivity of himbacine: a muscarine receptor antagonist. *Naunyn-Schmiedeberg's Arch. Pharmacol.* **332**:16–20 (1986).
27. Melchiorre, C., P. Angeli, G. Lambrecht, E. Mutschler, M. T. Picchio, and J. Wess. Antimuscarinic action of methoctramine, a new cardioselective M_2 muscarinic receptor antagonist, alone and in combination with atropine and gallamine. *Eur. J. Pharmacol.* **144**:117–124 (1987).
28. Birdsall, N., N. Buckley, H. Dodds, K. Fukuda, A. Giachetti, R. Hammer, H. Kilbinger, G. Lambrecht, E. Mutschler, N. Nathanson, A. North, and R.

[7] N. Buckley, unpublished observations.

Schwarz. Nomenclature for muscarinic receptor subtypes recommended by symposium. *Trends Pharmacol. Sci.* (Suppl 4.) VII (1989).
29. Kwatra, M. M., J. Ptasienski, and M. M. Hosey. The porcine heart M_2 muscarinic receptor: agonist-induced phosphorylation and comparison of properties with the chick heart receptor. *Mol. Pharmacol.* **35**:553–558 (1989).
30. Jeck, D., R. Lindmar, K. Loffelholz, and M. Wanke. Subtypes of muscarinic receptor on cholinergic nerves and atrial cells of chicken and guinea-pig hearts. *Br. J. Pharmacol.* **93**:357–366 (1988).
31. Choo, L. K., F. Mitchelson, and P. Napier. Differences in antagonist affinities at muscarinic receptors in chick and guinea-pig. *J. Auton. Pharmacol.* **8**:259–266 (1988).
32. Michel, A. D., and R. L. Whiting. Radioligand binding characteristics of the chicken cardiac muscarinic receptor. *Naunyn-Schmiedeberg's Arch. Pharmacol.* **340**:279–284 (1989).
33. Bloom, J. W., M. Halonen, L. J. Lawrence, E. Rould, N. A. Seaver, and H. I. Yamamura. Characterization of high affinity [^{3}H]pirenzepine and (−)-[^{3}H] quinuclidinyl benzilate binding to muscarinic cholinergic receptors in rabbit peripheral lung. *J. Pharmacol. Exp. Ther.* **240**:51–58 (1987).
34. Bloom, J. W., M. Halonen, and H. I. Yamamura. Characterization of muscarinic cholinergic receptor subtypes in human peripheral lung. *J. Pharmacol. Exp. Ther.* **244**:625–632 (1988).
35. McCormack, D. G., J. C. Mak, P. Minette, and P. J. Barnes. Muscarinic reecptor subtypes mediating vasodilation in the pulmonary artery. *Eur. J. Pharmacol.* **158**:293–297 (1988).
36. Mak, J. C. W., and P. J. Barnes. Muscarinic receptor subtypes in guinea-pig and human lung. *Br. J. Pharmacol.* **95**(suppl.):777P (1988).
37. Gies, J.-P., C. Bertrand, P. Vanderheyden, F. Waeldele, P. Dumont, G. Pauli, and Y. Landry. Characterization of muscarinic receptors in human, guinea-pig and rat lung. *J. Pharmacol. Exp. Ther.* **250**:309–315 (1989).
38. Bloom, J. W., H. I. Yamamura, C. Baumgartner, and M. Halonen. A muscarinic receptor with high affinity for pirenzepine mediates vagally induced bronchoconstriction. *Eur. J. Pharmacol.* **133**:21–27 (1987).
39. Maclagan, J., and D. Faulkner. Effect of pirenzepine and gallamine on cardiac and pulmonary muscarinic receptors in the rabbit. *Br. J. Pharmacol.* **97**:506–512 (1989).
40. Brown, J. H., and D. Goldstein. Analysis of cardiac muscarinic receptors recognized selectively by nonquaternary but not by quaternary ligands. *J. Pharmacol. Exp. Ther.* **238**:580–586 (1986).
41. Akiyama, K., M. Watson, W. R. Roeske, and H. I. Yamamura. High-affinity [^{3}H]pirenzepine binding to putative M_1 muscarinic sites in the neuroblastoma × glioma hybrid cell line (NG 108-15). *Biochem. Biophys. Res. Commun.* **119**:289–297 (1984).
42. Evans, T., M. M. Smith, L. I. Tanner, and T. K. Harden. Muscarinic cholinergic receptors of two cell lines that regulate cyclic AMP metabolism by different molecular mechanisms. *Mol. Pharmacol.* **26**:395–404 (1984).
43. Michel, A. D., R. Delmendo, E. Stefanich, and R. L. Whiting. Binding characteristics of the muscarinic receptor subtype of the NG108-15 cell line. *Naunyn-Schmiedeberg's Arch. Pharmacol.* **340**:62–67 (1989).
44. Michel, A. D., E. Stefanich, and R. L. Whiting. PC12 phaeochromocytoma cells contain an atypical muscarinic receptor binding site. *Br. J. Pharmacol.* **97**:914–920 (1989).
45. Giraldo, E., R. Micheletti, E. Montagna, A. Giachetti, M. A. Vigano, H. Ladinksy, and C. Melchiorre. Binding and functional characterization of the cardioselective muscarinic antagonist methoctramine. *J. Pharmacol. Exp. Ther.* **244**:1016–1020 (1988).
46. Eglen, R. M., W. W. Montgomery, I. A. Dainty, L. K. Dubuque, and R. L. Whiting. The interaction of methoctramine and himbacine at atrial, smooth muscle and endothelial muscarinic receptors in vitro. *Br. J. Pharmacol.* **95**:1031–1038 (1988).
7. Waelbroeck, M., J. Camus, M. Tastenoy, and J. Christophe. 80% of muscarinic receptors expressed by the NB-OK 1 human neuroblastoma cell line show high affinity for pirenzepine and are comparable to rat hippocampus M_1 receptor. *FEBS Lett.* **226**:287–290 (1988).
48. Nilvebrant, L., and B. Sparf. Receptor binding profiles of some selective muscarinic antagonists. *Eur. J. Pharmacol.* **151**:83–96 (1988).
49. Wang, J. X., W. R. Roeske, W. Wang, and H. I. Yamamura. Himbacine recognizes a high affinity subtype of M_2 muscarinic cholinergic receptors in the rat cerebral cortex. *Brain Res.* **446**:155–158 (1988).
50. Delmendo, R. E., A. D. Michel, and R. L. Whiting. Affinity of muscarinic receptor antagonists for three putative muscarinic receptor binding sites. *Br. J. Pharmacol.* **96**:457–464 (1989).
51. Takayanagi, I., F. Konno, M. Akaike, Y. Niibori, and S. Yamaura. *cis*(−)-2,3-Dihydro-3-(4-methylpiperazinylmethyl)-2-phenyl-1,5-benzothiazepin-4(5H)-one monohydrochloride and its butylbromide as M_1-receptor antagonists. *Gen. Pharmacol.* **18**:91–93 (1987).
52. Barlow, R. B., M. K. Shepherd, H. Tydeman, and M. A. Veale. The affinity of some acetylenic analogues of 4-DAMP methobromide for muscarinic receptors in guinea-pig ileum and atria. *Br. J. Pharmacol.* **94**:947–951 (1988).
53. Tietje, K. M., P. S. Goldman, and N. M. Nathanson. Cloning and functional analysis of a gene encoding a novel muscarinic acetylcholine receptor expressed in chick heart and brain. *J. Biol. Chem.* **265**:2828–2834 (1990).
54. Dietl, M. M., R. Cortes, and J. M. Palacios. Neurotransmitter receptors in the avian brain. II. Muscarinic cholinergic receptors. *Brain Res.* **439**:360–365 (1988).
55. Waelbroeck, M., M. Gillard, P. Robberecht, and J. Christophe. Kinetic studies of [^{3}H]-*N*-methylscopolamine binding to muscarinic receptors in the rat central nervous system: evidence for the existence of three classes of binding sites. *Mol. Pharmacol.* **30**:305–314 (1986).
56. Buckley, N. J., T. I. Bonner, and M. R. Brann. Localization of a family of muscarinic receptor mRNAs in rat brain. *J. Neurosci.* **8**:4646–4652 (1988).
57. Bennet, J. P., Jr. Methods in binding studies. in *Neurotransmitter Receptor Binding* (H. I. Yamamura, S. J. Enna, and M. J. Kuhar, eds). Raven Press, New York, 57–90 (1978).

Send reprint requests to: Dr. Sebastian Lazareno, MRC Collaborative Centre, 1–3 Burtonhole Lane, Mill Hill, London, NW7 1AD, UK.